

Vanillic Mannich bases: synthesis and screening of biological activity. Mechanistic insight into the reaction with 4-chloroaniline†

Cite this: *RSC Adv.*, 2014, 4, 24635

Vladimir P. Petrović,^{*a} Dušica Simijonović,^a Marko N. Živanović,^b Jelena V. Košarić,^b Zorica D. Petrović,^a Svetlana Marković^a and Snežana D. Marković^b

One-step multi-component Mannich reaction of vanillin, aromatic amines (aniline and 4-chloroaniline), and cyclohexanone was successfully catalyzed by three chloroacetate ethanolamine based ionic liquids: diethanolammonium chloroacetate, and newly synthesized ethanolammoniumchloroacetate and *N,N*-diethylethanolammoniumchloroacetate. These reactions were performed in ethanol at room temperature. Mechanistic aspects of the reaction with 4-chloroaniline were considered by using density functional theory. The yield of obtained Mannich bases (**MB-Cl** and newly synthesized **MB-H**) was very good, while diastereoselectivity was excellent. These compounds were evaluated for their *in vitro* antioxidative activity by DPPH free radical scavenging assay. It was shown that both bases exhibit high activity against DPPH. *In vitro* cytotoxic and antioxidative effects of **MB-Cl** and **MB-H** against human breast carcinoma MDA-MB-231 and human colon carcinoma HCT-116 cell lines were also determined. The investigated Mannich bases show moderate or very weak cytotoxic effect on HCT-116 cells, while no cytotoxic effect was observed in the case of MDA-MB-231 cells. On the other hand, the tested substances induced oxidative stress in the treated cancer cell lines.

Received 29th April 2014
Accepted 27th May 2014

DOI: 10.1039/c4ra03909b

www.rsc.org/advances

Introduction

The Mannich-type reaction is one of the very important strategies in the production of chiral compounds. The final product of this reaction is a β -amino-carbonyl compound, also known as a Mannich base. The traditional catalysts for classical Mannich reaction of aldehydes, ketones and amines involve mainly Lewis acids,¹ Lewis bases,² Brønsted acids,³ rare metal salts,⁴ and organocatalysts.⁵ However, the usage of these catalysts has a number of serious disadvantages, such as harsh reaction conditions, toxicity and difficulty in separation of products. All these problems limit their usage, especially when it comes to the synthesis of the complex molecules. Ionic liquids proved to be a promising alternative to the conventional catalysts.⁶ They were initially introduced as alternative green reaction media, but today they play numerous roles. Ionic liquids, based on the Brønsted and Lewis acids, exhibit a great potential in replacement of conventional homogeneous and heterogeneous acidic catalysts. These substances have been successfully applied to a

variety of reactions including the Diels–Alder reaction,⁷ Mannich reaction,^{6,8} Friedel–Crafts reaction,⁹ aldol condensation,¹⁰ and esterification.¹¹

Mannich bases are structural fragments of many biologically active compounds and pharmaceutical products, such as nucleotides, peptides, alkaloids, steroid hormones, antibiotics, and vitamins.¹² These compounds show a wide range of bioactivities, such as antitubercular,¹³ antimalarial,¹⁴ vasorelaxing,¹⁵ anticancer,¹⁶ analgesic,¹⁷ anti-inflammatory,¹⁸ antifungal,¹⁹ antioxidative,²⁰ *etc.*

In this paper, one-pot multi-component Mannich reaction, which leads to the highly functionalized vanillin derivatives, is presented. The reaction was catalysed with chloroacetate ethanolamine based salts. As these substances are liquid at room temperature, they belong to the class of ionic liquids (ILs). To our best knowledge, there are no literature data on the mechanism of Mannich reaction catalysed with this type of ILs. In addition, cytotoxic effects of Mannich bases on cancer cells have been only little investigated. Thus, our investigation had two additional goals: to provide a mechanistic insight *via* the model reaction of vanillin, 4-chloroaniline and cyclohexanone, and to test the obtained Mannich bases for possible cytotoxic and antioxidative activities.

Results and discussion

The one-pot Mannich reactions of vanillin, aromatic amine (aniline or 4-chloroaniline), and cyclohexanone were carried out

^aFaculty of Science, University of Kragujevac, Department of Chemistry, RadojaDomanovića 12, 34000 Kragujevac, Serbia. E-mail: vladachem@kg.ac.rs; Fax: +38134335040

^bFaculty of Science, University of Kragujevac, Department of Biology and Ecology, RadojaDomanovića 12, 34000 Kragujevac, Serbia

† Electronic supplementary information (ESI) available: Characterization of **MB-H** and **MB-Cl** (¹H, ¹³C NMR and ESI-MS spectra). See DOI: 10.1039/c4ra03909b

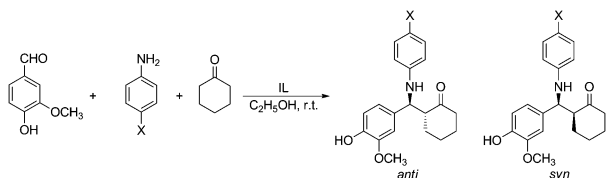
in the presence of catalytic amount (15 mol%) of chloroacetate ethanolamine based salts (ILs): diethanolammonium chloroacetate ([HDEA][ClAc]), and newly synthesized ethanolammoniumchloroacetate ([HMEA][ClAc] and *N,N*-diethylethanolammoniumchloroacetate ([HDEAE][ClAc]). To confirm catalytic action of the applied salts, some control experiments were performed: blank experiments, and those catalyzed with a common ammonium salt, triethylethanolammonium chloride [Et₃NH][Cl] (reactions 5 and 10 in Table 1). The reactions were performed in ethanol at room temperature, and monitored by ¹H NMR spectroscopy. Among used ILs, it was found that [HDEA][ClAc] was the most effective catalyst for these conversions. The obtained results showed that the yield of the Mannich products was generally very good, although vanillin possesses deactivating groups. In addition, diastereoselectivity of the obtained products was excellent (Table 1). After recrystallization, spectral analysis of the obtained products by ¹H NMR, ¹³C NMR, IR spectroscopy, and ESI-MS spectrometry was conducted. It was shown that 2-[1-(4-chlorophenylamino)-1-(4-hydroxy-3-methoxyphenyl)]methylcyclohexanone (**MB-CI**) and 2-[1-(*N*-phenylamino)-1-(4-hydroxy-3-methoxyphenyl)]methylcyclohexanone (**MB-H**) are the products of the reactions 2–5, and 7–10, respectively. By comparing our results to the literature data,²¹ we concluded that only *syn* isomer of **MB-CI** was obtained, while in the case of **MB-H** only *anti* isomer was found (Table 1). This conclusion is based on the chemical shifts and coupling constants of the signals corresponding to the –CH–N proton. Namely, the *syn* diastereoisomer exhibits a higher δ value and lower J value (d , $\delta = 4.62$, $J = 4.4$ Hz), while the *anti* isomer possesses a lower δ value and

higher J value (d , $\delta = 4.54$, $J = 7.4$ Hz). It is worth pointing out that, based on the ¹H NMR spectra of the crude reactions mixtures, the *anti* isomer was not detected in the reactions with 4-chloroaniline, and the *syn* isomer was not identified in the reactions with aniline. As can be seen from Table 1, the uncatalyzed reactions did not occur at all, while in the presence of [Et₃NH][Cl] the yield of the desired Mannich products was low, and stereoselectivity poor.

A DFT study was performed to examine the mechanism of the Mannich reaction of vanillin, 4-chloroaniline, and cyclohexanone catalysed with chloroacetate ethanolamine based salts. Since our experimental results undoubtedly showed that only *syn* isomers of **MB-CI** are yielded in the reactions, our computational efforts were focused on the elucidation of the *syn* reaction pathway. In accord with our experiments, we analysed the same reaction in the presence of the common catalyst [Et₃NH][Cl].

The first part of the reaction, a nucleophilic attack of the 4-chloroaniline nitrogen at the carbonyl group of vanillin, provides the formation of the α -amino alcohol **Int-1** (Fig. S1†). Fig. 1 presents further mechanistic transformations of the reaction catalysed with [HDEA][ClAc], whereas the figures concerning other two ILs are given in ESI.† Firstly, **Int-1** is protonated by the diethanolammonium ion from [HDEA][ClAc]. After dehydration of the protonated amino alcohol, the iminium ion **Int-3** is formed. In the further course of the reaction, the enol form of cyclohexanone attacks C_v carbon of the iminium ion, forming the protonated Mannich base **Int-5**. The hydrogen atom bonded to O_e of **Int-5** spontaneously moves

Table 1 Mannich reaction catalysed by different chloroacetate ethanolamine based salts^a



Entry	Amine		Yield (%)	<i>anti</i> : <i>syn</i>
	X	Catalyst		
1	Cl	—	n.r.	—
2	Cl	[HDEA][ClAc]	87	0 : 100
3	Cl	[HMEA][ClAc]	82	0 : 100
4	Cl	[HDEAE][ClAc]	78	0 : 100
5	Cl	[Et ₃ NH][Cl]	32	46 : 54
6	H	—	n.r.	—
7	H	[HDEA][ClAc]	89	100 : 0
8	H	[HMEA][ClAc]	86	100 : 0
9	H	[HDEAE][ClAc]	84	100 : 0
10	H	[Et ₃ NH][Cl]	41	51 : 49

^a Reaction conditions: aldehyde:amine:ketone, 1 : 1 : 1.5 (mole ratio); temperature = room temperature; n.r. = no reaction; catalyst (15 mol%); ethanol as solvent (1 mL).

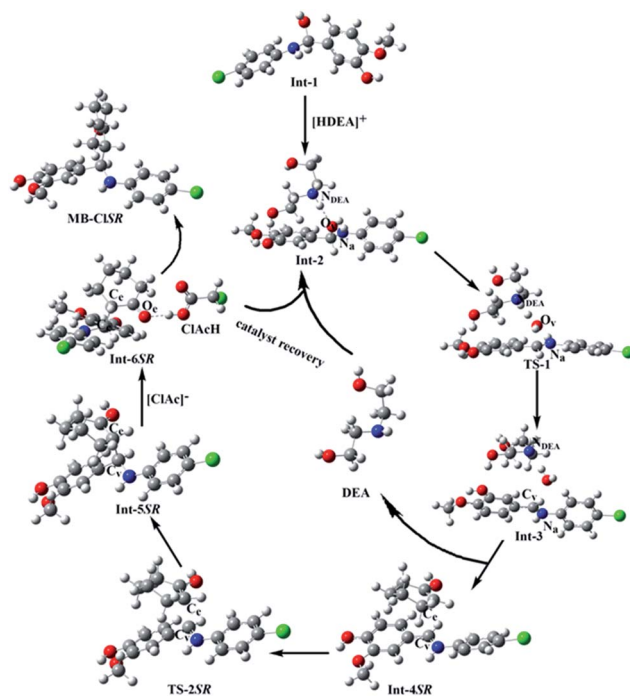


Fig. 1 The proposed catalytic cycle for the Mannich reaction of vanillin, 4-chloroaniline and cyclohexanone catalyzed with [HDEA][ClAc].

to the chloroacetic anion of the catalyst, yielding the final product of the reaction **MB-ClSR**. It is worth pointing out that both precursors of IL (diethanolamine and ClAcH) are liberated in the course of the reaction, implying that the overall reaction provides the catalyst recovery. This finding is supported with our experiments, which showed that the usage of the recovered catalysts was successful.

Our assumption that the first step of the reaction is a nucleophilic attack of the 4-chloroaniline nitrogen at the carbonyl group of vanillin is supported with the HOMO of 4-chloroaniline and LUMO of vanillin (Fig. S2†). It is shown that the most electron sufficient area in 4-chloroaniline is nitrogen atom N_a (NBO charge = -0.819), while the most electron deficient area of vanillin is carbon atom from carbonyl group C_v (NBO charge = 0.459). Due to achiral reaction environment, one can expect that both *R* and *S* isomers will be equally formed. This assumption was confirmed by revealing the transition states **TS-S** and **TS-R** (Fig. S1†) which require activation energies of 154.2 and 157.0 kJ mol $^{-1}$. In these transition states, the new N_a-C_v and O_v-H bonds are being formed, while the N_a-H bond is broken. Our discussion will be focused on the transformations of the *S* isomer catalysed with [HDEA][ClAc], whereas the corresponding details on the *R* isomer, as well as transformations catalysed with the other two catalysts are presented ESI (Fig. S3 and S4, Table S1)†.

The reaction further proceeds in the presence of the IL catalyst. Bearing in mind that our reactions were carried out in ethanol as solvent, and that ethanolamine based ILs behave as separated ions in polar solvents,²² it can be expected that diethanolammonium cations and chloroacetic anions were present in the reaction mixture. Our DFT study showed that [HDEA] $^+$, the cationic part of IL, forms hydrogen bonds with **Int-1**, yielding **Int-2** (Fig. 1). These hydrogen bonds are formed *via* an OH group from the cation and the phenolic oxygen from **Int-1** (OH \cdots O, 1.994 Å), and *via* the $N_{DEA}-H$ bond from the diethanolammonium ion and O_v (NH \cdots O, 1.831 Å). The NBO analysis confirms that there is donation of electron density from the lone pair on O_v to the antibonding $\sigma^* N_{DEA}-H$ orbital, as well as from the lone pair on the phenolic oxygen to the antibonding $\sigma^* O-H$ orbital from the [HDEA] $^+$ moiety.

Upon hydrogen bonds establishing, the reaction occurs through the transition state **TS-1**, where the concerted cleavage of the $N_{DEA}-H$ and C_v-O_v bonds, and transfer of the proton to O_v take place. This implies that DEA, the precursor of [HDEA]-[ClAc], and water molecule are liberated in this phase of the reaction. In this way, **Int-3** is formed, with the imminium ion as a constituent (Fig. 1).

As for the further course of the reaction, we assumed that cyclohexanone tautomerizes into the enol form, and attacks C_v of the imminium ion. This assumption is supported with the NBO charges on C_v from the imminium ion (0.283) and C_e from the enol form of cyclohexanone (-0.310). In addition, the LUMO of the imminium ion and HOMO of the enol delineate electron most deficient (C_v) and electron most sufficient (C_e) areas in these molecules (Fig. S5†). There are four possible ways for this attack, depending on the orientation of the enol and imminium ion, implying that there are four possible reactant

complexes: **Int-4SR** (Fig. 1), **Int-4RS**, **Int-4SS**, and **Int-4RR** (Fig. S6†). Each of these structures is stabilized by electrostatic interaction between C_v and C_e , as well as by the hydrogen bond formed from H bonded to N_a of the imminium ion and O_e from the enol. The transition states **TS-2** were revealed (**TS-2SR**, **TS-2RS**, **TS-2SS**, and **TS-2RR**), where a new carbon-carbon bond (C_v-C_e) is being formed, while both π bonds (from the imminium ion and enol) are being cleaved. In this stage of the reaction, leading to the formation of **Int-5**, C_v and C_e become chiral. Namely, in **TS-2SR** C_e and C_v adopt the *S* and *R* configurations (and respective configurations in other molecules of **TS-2**). In all intermediates **Int-5** the new σC_v-C_e bond is completely formed, while both π bonds are completely broken. O_e is still protonated. Until this point both catalysts behave in the same manner. In the case of ILs the next step of the reaction is a spontaneous deprotonation of **Int-5** by the chloroacetic anion (**Int-6**), leading to the liberation of the reaction product **MB-Cl** and ClAcH. It is now clear that both precursors of the catalyst are yielded. On the other hand, when [Et $_3$ NH][Cl] was used as catalyst, the proton transfer from **Int-5** to the chloride anion does not occur, either spontaneously, or *via* a transition state. Such behaviour of this weak base is not surprising. It is reasonable to expect that the liberated Et $_3$ N takes the role of a proton acceptor.

The energetics of the examined reactions is presented in Table 2. The top of the table contains the results for the first part of the cycle (up to **Int-3**), which is characteristic for each IL. The bottom of the table contains the results for the second part of the cycle (from **Int-4**), which is identical for all catalysts.

A comparison of the data presented in Table 2 and those for the nucleophilic attack of the 4-chloroaniline nitrogen at the carbonyl group of vanillin reveals that the formation of **Int-1** is the rate determining step of the overall examined reactions. Since this reaction step is independent of the catalyst used, it does not influence the reaction yields. The energy profiles of the catalytic cycle (Table 2) clearly indicate that the protonation of **Int-1** and formation of the new carbon-carbon bond are endothermic and slow steps, while the spontaneous proton shift from **Int-5** to [ClAc] $^-$ is highly exothermic and fast. As a consequence, the overall catalytic cycle is slightly exothermic. This finding is agreement with the experimental fact that the

Table 2 Energy profiles for the examined catalyzed reactions. The free energy values (kJ mol $^{-1}$) were calculated relative to **Int-2**

Catalyst	Int-2	TS-1	Int-3		
[HDEA][ClAc]	0	62.6	21.6		
[HMEA][ClAc]	0	64.5	19.5		
[HDEAE][ClAc]	0	70.3	37.2		
	Int-4	TS-2	Int-5	Int-6	MB-Cl
<i>SR</i>	13.3	55.8	41.0	-82.2	-108.6
<i>RS</i>	11.6	58.1	39.6	-84.5	-96.8
<i>SS</i>	16.7	64.4	41.6	-80.7	-114.5
<i>RR</i>	9.8	61.0	47.8	-81.0	-94.9

reaction occurs at room temperature. The protonation of **Int-1** is the rate determining step of the catalytic cycle. The activation energies for this reaction step in the presence of different catalysts are inversely proportional to the experimentally obtained yields (Table 1).

As for the conversion of **Int-1R** catalyzed with the same ILs, we found practically identical mechanistic and energetic results (Fig. S4 and Table S1†).

Antioxidative activity by DPPH assay

The DPPH free radical scavenging activity of **MB-H** and **MB-Cl** is shown in Table 3. Both investigated compounds interact well with DPPH, and exhibit high activity, slightly lower than the reference compound NDGA, and can be considered as good antioxidants. This interaction can be attributed to the common behaviour of phenolic compounds.

Encouraged by these results, *in vitro* antioxidative and cytotoxic effects of **MB-Cl** and **MB-H** on the human cancer cells were also evaluated.

Biological evaluation

Cytotoxic effect. The cell viability was followed by MTT assay.²³ Our results showed that **MB-H** and **MB-Cl** exert moderate cytotoxic effect on HCT-116 cells, and no cytotoxic effect on MDA-MB-231 cells (Table 4). It should be emphasized that the starting compounds (4-chloroaniline, aniline, vanillin, and cyclohexanone) showed no cytotoxic effect on both cell lines (Fig. S7 and S8†). According to the obtained results, **MB-H** showed the greatest cytotoxic effect on HCT-116 cells ($IC_{50} = 251 \pm 4.1$ and $99 \pm 3.7 \mu\text{M}$ for 24 h and 72 h respectively). Cell viability gradually decreased with the increasing substance concentration. **MB-H** was more effective 72 h after the treatment, in comparison to 24 h. The shape of dose-response

curves of **MB-H** and **MB-Cl** indicates inhibition of cell growth mainly at the highest concentrations applied (Fig. S9†). The greatest influence of the investigated compounds on cell viability of HCT-116 cells is in agreement with our previous investigations, which proved that MDA-MB-231 cells, as metastatic, invasive cancer cells, are more stable and more resistant to chemicals than HCT-116 cells.²⁴

Prooxidative/antioxidative effects

Determination of superoxide anion radical ($O_2^{\cdot-}$). The concentration of $O_2^{\cdot-}$, the most potent reactive oxygen species (ROS) and indicator of oxidative stress, was determined by spectrophotometric method.²⁵ Evaluation of $O_2^{\cdot-}$ content in HCT-116 and MDA-MB-231 cells was performed after 24 and 72 h from the treatment. The effects of **MB-H** and **MB-Cl** on HCT-116 and on MDA-MB-231 cells are presented in Table 5. Both compounds increased the $O_2^{\cdot-}$ content, especially after 24 h, with statistically significant difference from the control cells. These results indicate acute oxidative stress appearance in the treated cells. **MB-H** induced greater increase of the $O_2^{\cdot-}$ concentration compared to **MB-Cl**. The increase of the $O_2^{\cdot-}$ concentration is greater on HCT-116 than on MDA-MB-231 cells.

Determination of nitrites (NO_2^-). The spectrophotometric determination of nitrites was performed by using the Griess method. Concentration of nitrites indicates quantity of nitrosonium ions (NO^+) in anaerobic conditions. In water, the final product of aerobic phase reaction between NO and O_2 is nitrogen dioxide (NO_2), which quickly combines with excess of NO, forming N_2O_3 that is hydrolysed to nitrite.²⁶ So, nitrite concentration may indicate of the levels of NO and reactive nitrogen species (RNS) in cells. The results obtained on the investigated cells showed significant change in the NO_2^- content after 24 h, as well as after 72 h from the treatments (Table 6).

Our results obtained on HCT-116 cells showed that **MB-H** induces the increase of the NO_2^- content. This increase is large after both treatment periods. Similarly, **MB-Cl** exerted the increase of the NO_2^- concentration after 24 h, while after 72 h the increase was not statistically significant. We even observed statistically significant decrease of the NO_2^- content at lower concentrations of **MB-Cl**. **MB-H** and **MB-Cl** showed different influence to the NO_2^- level on MDA-MB-231 cell line. Similarly to the results obtained on HCT-116, **MB-H** induced the increase of the NO_2^- content. On the other hand, **MB-Cl** showed significant lowering of the NO_2^- concentration after 24 h, but significant increasing after 72 h.

On the basis of the obtained results one can conclude that elevation of the $O_2^{\cdot-}$ and NO_2^- levels indicates oxidative stress appearance in the treated cells, and can be the cause of cytotoxic effects of **MB-H** on HCT-116 cells.²⁷

Determination of reduced glutathione (GSH)

The GSH is a tripeptide which is representing a primary antioxidative defence of eukaryotic cell. Table 7 represents the influence of **MB-H** and **MB-Cl** on the GSH content in HCT-116 and MDA-MB-231 cells.

Table 3 Interaction of the examined and reference compounds with the stable free radical DPPH

Concentration (μM)	Inhibition (%)					
	MB-H		MB-Cl		NDGA	
	20 min	60 min	20 min	60 min	20 min	60 min
100	89.8	91.6	90.9	92.1	96.2	96.2
50	83.6	89.6	87.9	91.7	94.8	95.9
25	72.3	84.9	78.7	86.9	94.1	95.4
IC_{50} (μM)	11.3		14.5			

Table 4 Growth inhibitory effects of the investigated compounds on HCT-116 and MDA-MB-231 cell lines (IC_{50} , μM)

Tested substance	HCT-116		MDA-MB-231	
	24 h	72 h	24 h	72 h
MB-H	251.0 ± 4.1	99.0 ± 3.7	>500.0	>500.0
MB-Cl	>500.0	330.0 ± 8.3	>500.0	>500.0

Table 5 Effects of MB-H and MB-Cl on HCT-116 and MDA-MB-231 cell lines, expressed as the $O_2^{\cdot-}$ concentration, after 24 and 72 h of exposure. * $p < 0.05$ as compared to the control cells

Superoxide anion radical, $O_2^{\cdot-}$ (nmol mL ⁻¹)				
Concentration	MB-H		MB-Cl	
	24 h	72 h	24 h	72 h
HCT-116				
0 μ M	33.92 \pm 0.25	27.2 \pm 0.26	33.92 \pm 0.25	27.2 \pm 0.26
1 μ M	40.51 \pm 0.45*	26.32 \pm 0.73	31.41 \pm 0.28	25.23 \pm 0.21*
10 μ M	45.63 \pm 1.65*	24.29 \pm 0.49*	38.48 \pm 0.29*	22.59 \pm 0.21*
50 μ M	39.6 \pm 1.65*	26.16 \pm 0.18	38.00 \pm 1.39*	25.65 \pm 0.37*
100 μ M	44.19 \pm 0.80*	29.57 \pm 0.82*	37.15 \pm 1.37*	30.69 \pm 0.26*
MDA-MB-231				
0 μ M	25.54 \pm 0.36	24.98 \pm 0.25	25.54 \pm 0.36	24.98 \pm 0.25
1 μ M	26.05 \pm 0.07	28.05 \pm 0.77*	27.76 \pm 0.12*	25.49 \pm 0.03
10 μ M	26.83 \pm 0.10*	29.87 \pm 1.02*	26.83 \pm 0.39	24.03 \pm 0.07*
50 μ M	26.72 \pm 0.32*	26.13 \pm 1.25	27.09 \pm 0.46	25.23 \pm 0.35
100 μ M	28.4 \pm 0.32*	26.05 \pm 0.42	27.15 \pm 1.43	24.05 \pm 0.42*

Table 6 Effects of MB-H and MB-Cl on HCT-116 and MDA-MB-231 cell lines, expressed as the NO_2^- concentration, after 24 and 72 h of exposure. * $p < 0.05$ as compared to the control cells

Nitrite, NO_2^- (nmol mL ⁻¹)				
Concentration	MB-H		MB-Cl	
	24 h	72 h	24 h	72 h
HCT-116				
0 μ M	161.1 \pm 6.83	159.73 \pm 4.11	161.1 \pm 6.83	159.73 \pm 4.11
1 μ M	93.82 \pm 3.49*	225.73 \pm 7.86*	89.46 \pm 4.11*	56.73 \pm 1.58*
10 μ M	200.51 \pm 6.20*	200.81 \pm 0.90*	233.03 \pm 3.73*	123.41 \pm 4.55*
50 μ M	195.44 \pm 7.55*	225.84 \pm 2.00*	199.39 \pm 6.23*	174.67 \pm 17.9
100 μ M	146.3 \pm 4.05	232.12 \pm 3.35*	227.56 \pm 2.26*	132.32 \pm 16.72
MDA-MB-231				
0 μ M	108.00 \pm 7.00	173.86 \pm 2.15	108.00 \pm 7.00	173.86 \pm 2.15
1 μ M	74.47 \pm 1.52*	184.91 \pm 2.81	52.48 \pm 7.34*	71.84 \pm 2.81*
10 μ M	171.43 \pm 2.74*	228.37 \pm 1.34*	56.13 \pm 0.56*	201.92 \pm 3.09*
50 μ M	101.62 \pm 6.07	186.32 \pm 1.53	86.02 \pm 3.16*	227.76 \pm 2.72*
100 μ M	141.03 \pm 3.11*	224.01 \pm 13.33*	67.78 \pm 3.50*	146.61 \pm 10.34*

MB-H showed no significant change in the GSH level on HCT-116 cells. It was shown that at low concentrations of MB-H the GSH level was slightly decreased after 24 and 72 h. Similarly, the decrease was observed with MB-Cl after 24 h, while after 72 h statistically significant increase of the GSH level was noticed. On the other hand, both substances caused large increase of the GSH level on MDA-MB-231 cells after both treatment periods. Larger increase in the GSH level was observed with MB-Cl. The elevation of the GSH level can be explained as follows. Firstly, as an answer to the induced oxidative stress, *de novo* synthesis of GSH can be induced.²⁸ Secondly, antioxidative action of the tested Mannich bases may preserve endogenous antioxidative capacity of GSH. In addition, our results showed higher GSH level in MDA-MB-231 cells (compared to HCT-116 cells) after the treatment by both MB-H and MB-Cl. This occurrence indicates

better redox equilibrium in these cells, and consequently, less cytotoxicity of the tested compounds.

Bearing in mind the obtained results for biological activities of the investigated Mannich bases, one can observe moderate cytotoxic effects on HCT-116 cells, and no cytotoxic effects on MDA-MB-231 cells. Also, it can be noticed that both compounds showed a disequilibrium prooxidative/antioxidative action. MB-H shifts equilibrium to the direction of prooxidative behaviour, *i.e.* induces oxidative stress on the investigated cells. On the other hand, MB-Cl shifts equilibrium to the direction of antioxidative behaviour. Larger cytotoxicity of MB-H towards HCT-116 cells, compared to MB-Cl, is in agreement with the redox status of these cells, mainly because of larger production of $O_2^{\cdot-}$ and NO_2^- . It was shown that the increased levels of ROS and RNS significantly contribute to cytotoxicity.²⁷ In addition,

Table 7 Effects of **MB-H** and **MB-Cl** on HCT-116 and MDA-MB-231 cell line after 24 and 72 h of exposure on the reduced glutathione (GSH) content expressed as nmol mL⁻¹. **p* < 0.05 as compared with control

Glutathione, GSH (nmol mL ⁻¹)				
Concentration	MB-H		MB-Cl	
	24 h	72 h	24 h	72 h
HCT-116				
0 μM	18.35 ± 0.45	15.44 ± 0.65	18.35 ± 0.45	15.44 ± 0.65
1 μM	17.51 ± 0.10*	14.16 ± 0.18	17.13 ± 0.07*	18.53 ± 0.92*
10 μM	17.62 ± 0.09*	14.82 ± 0.62	17.98 ± 0.06	17.03 ± 0.16
50 μM	18.37 ± 0.18	15.16 ± 0.29	17.75 ± 0.06*	17.79 ± 0.60*
100 μM	18.7 ± 0.08	13.89 ± 0.34*	17.9 ± 0.10	16.26 ± 0.79
MDA-MB-231				
0 μM	25.94 ± 1.94	19.84 ± 0.41	25.94 ± 1.94	19.84 ± 0.41
1 μM	33.99 ± 3.91*	27.03 ± 0.09*	36.2 ± 0.85*	20.89 ± 0.36
10 μM	29.25 ± 0.50	31.04 ± 2.25*	39.64 ± 3.64*	25.44 ± 0.69*
50 μM	27.98 ± 1.22	24.84 ± 1.23*	40.98 ± 0.33*	21.42 ± 0.13
100 μM	27.4 ± 0.61	24.12 ± 0.94*	36.07 ± 0.86*	27.62 ± 1.29*

the GSH content, as antioxidative capacity, in the cells treated with **MB-H** is lower than in those treated with **MB-Cl**, and also may contribute to **MB-H** cytotoxicity.

A prooxidative action of the investigated compounds is not surprising. Namely, organic compounds containing phenolic²⁹ and alkoxy groups,³⁰ when present in cells, can exhibit both antioxidative and prooxidative activities.

As mentioned above, these results are in agreement with our earlier findings that HCT-116 cells are more sensitive to bioactive substances than MDA-MB-231 cells.²⁴ This result is also well described by the fact that these cell lines are of various types and source,³¹ *i.e.* HCT-116 cells line is of primary origin, while MDA-MB-231 is a metastatic tumour. On the other hand, the larger GSH level in MDA-MB-231 cells implies the lowering of the influence of ROS and RNS to the stability of the treated cells.

Conclusions

Chloroacetate ethanolamine based salts: [HDEA][ClAc], and new [HMEA][ClAc] and [HDEAE][ClAc] proved to successfully catalyse synthesis of the vanillic Mannich bases (**MB-Cl** and new **MB-H**) in one-pot reaction in very good yields. Only *syn* **MB-Cl** and *anti* **MB-H** were obtained, implying that diastereoselectivity of the reaction was excellent. Our DFT study showed that the overall catalytic cycle is slightly exothermic. This computational finding is in accord with the mild reaction conditions. The protonation of the α -amino alcohol intermediate is the rate determining step of the catalytic cycle. The activation energies for this reaction step in the presence of different catalysts are in agreement with the experimentally obtained yields.

DPPH free radical scavenging assay indicates that both Mannich bases interact well with DPPH, exhibit high activity, and can be considered as good antioxidants. Our biological investigations showed that both compounds induce acute oxidative stress of cancer cell lines, and also show enhanced antioxidative action with extended treatment time. **MB-H**

exhibits larger prooxidative, and thus cytotoxic effects, whereas **MB-Cl** exhibits higher antioxidative activity. Due to different origin of the investigated cancer cell lines, HCT-116 cells are more sensitive to the investigated Mannich bases than MDA-MB-231 cells.

The obtained results indicate direction of chemical transformations, which would lead towards synthesis of novel Mannich bases with more efficient cytotoxic and/or antioxidative actions.

Experimental section

Materials and reagents

The compounds chloroacetic acid, vanillin, aniline, 4-chloroaniline, cyclohexanone, nordihydroguareric acid (NDGA), and 2,2-diphenyl-1-picrylhydrazyl (DPPH) were obtained from Aldrich Chemical Co. MEA, DEA, and *N,N*-diethylethanolamine (DEAE) were purchased from Fluka. All common chemicals were of reagent grade. The IR spectra were recorded on a Perkin-Elmer Spectrum One FT-IR spectrometer using the thin film technique and KBr plates. The ¹H NMR and ¹³C NMR spectra were run in CDCl₃ on a Varian Gemini 200 MHz spectrometer. High-resolution LC/ESI TOF mass spectra were measured on a HPLC instrument (Agilent 1200 Series, Agilent Technologies) with a Zorbax Eclipse Plus C column (150 × 4.6 mm i.d.; 1.8 μm) and a diode-array detector (DAD) coupled with a 6210 time-of-flight LC/MS system (Agilent Technologies). Melting points were determined on a Mel-Temp capillary melting points apparatus, model 1001. Elemental microanalyses for carbon, hydrogen, and nitrogen were performed at the Faculty of Chemistry, University of Belgrade.

Dulbecco's Modified Eagle Medium (DMEM) and PBS were obtained from GIBCO, Invitrogen, USA. 5,5'-Dithio-bis(2-nitrobenzoic acid) was purchased from Sigma Chemicals Co., St Louis, MO, USA. Fetal bovine serum (FBS) and trypsin-EDTA were from PAA (The Cell Culture Company, Pasching, Austria).

Dimethyl sulfoxide (DMSO), 3-[4,5-dimethylthiazol-2-yl]-2,5-diphenyltetrazolium bromide (MTT), and nitro blue tetrazolium (NBT) were obtained from SERVA, Heidelberg, Germany. *N*-1-Naphthylethylenediamine dihydrochloride was purchased from Flukachemie GMBH, Buchs, Switzerland. Sulphanilamide and sulphanilic acid were purchased from MP Hemija Belgrade, Serbia. All solvents and chemicals were of analytical grade.

Ionic liquid synthesis

Three different ionic liquids were investigated. Diethanolammonium chloroacetate [HDEA][ClAc], was synthesized recently,²² while the other two, ethanolammoniumchloroacetate [HMEA][ClAc] and *N,N*-diethylethanolammoniumchloroacetate [HDEAE][ClAc] are newly synthesized.

General method

Ethanolammoniumchloroacetate and *N,N*-diethylethanolammoniumchloroacetate were prepared by dropping the stoichiometric amount of chloroacetic acid to the dichloromethane-ethanol solution of corresponding amino alcohol (ethanolamine or *N,N*-diethylethanamine). The reaction mixture was stirred during 2 h at room temperature. After completion of the reaction, the resulting solution was evaporated under the reduced pressure. The residue was dried in vacuum at 50 °C for 4 h to generate the corresponding product. The prepared ILs are colourless viscous liquids.

Spectral characterization of the ionic liquids: ¹H NMR spectrum (200 MHz, CDCl₃): [HMEA][ClAc]: δ = 3.21 (t, 2H) ppm; 3.86 (t, 2H) ppm; 4.14 (s, 2H). IR (film): ν = 2953, 1585, 1393, 1064, 776 cm⁻¹; [HDEAE][ClAc]: δ = 1.42 (t, 6H) ppm; 3.19 (q, 4H) ppm; 3.23 (t, 2H) ppm; 4.01 (t, 2H) ppm; 4.13 (s, 2H). IR (film): ν = 3244, 2984, 1607, 1380, 1243, 1082, 766 cm⁻¹.

General procedure for Mannich reaction

Vanillin (1 mmol), amine (aniline or 4-chloroaniline) (1 mmol), cyclohexanone (1.5 mmol), chloroacetate ethanolamine based salt as catalyst (15 mol%) and 1 mL of ethanol were placed in flask and stirred at room temperature for 24 h. After completion of the reaction, the solid product was separated by filtration and washed with ethanol. Upon the evaporation of the solvent, the remained catalyst was used in new experiments. It is worth to emphasize that there was no significant loss in the recycled catalyst activity, *i.e.* the yields were up to 5% lower. The control experiments were performed in the presence of triethylethanomammonium chloride as catalyst. The Mannich bases were obtained by recrystallization from dichloromethane and propanol (2 : 1) and analysed by ¹H NMR, ¹³C NMR, IR spectroscopy, and ESI-MS spectrometry.

2-[1-(*N*-4-Chlorophenylamino)-1-(4-hydroxy-3-methoxyphenyl)]-methylcyclohexanone (**MB-Cl**) (*syn* only, entry 1–3, Table 1): white crystals – Mp 160–161 °C; ¹H NMR (200 MHz, CDCl₃): 1.61–2.02 (m, 6H), 2.20–2.42 (m, 2H), 2.65–2.69 (m, 1H), 3.84 (s, 3H), 4.62 (d, *J* = 4.40 Hz, 1H), 5.54 (br s, 1H), 6.48 (d, *J* = 8.9 Hz, 2H), 6.78–6.87 (m, 3H), 7.01 (d, *J* = 8.8 Hz, 2H); ¹³C NMR (50 MHz, CDCl₃) δ: 24.8, 26.9, 28.8, 42.4, 55.9, 56.4, 57.6, 110.0, 114.1, 115.2, 120.3, 122.4, 128.8, 132.8, 144.6, 146.1, 146.6, 211.7; IR (cm⁻¹):

3387, 3152, 2926, 2859, 1701, 1601, 1501, 1402, 1320, 1171, 1091, 807, 709, 551; C₂₀H₂₂NO₃Cl (FW = 359.85): C, 66.75; N, 3.89; H, 6.16%; found: C, 66.77; N, 3.85; H, 6.19%; ESI-MS: *m/z* 358.1 [M – H]⁻; 2-[1-(*N*-phenylamino)-1-(4-hydroxy-3-methoxyphenyl)]methylcyclohexanone (**MB-H**) (*anti* only, entry 4–6, Table 1): colourless crystals – Mp 164–165 °C; ¹H NMR (200 MHz, CDCl₃): 1.67 (m, 2H), 1.83–1.89 (m, 4H), 2.37–2.41 (m, 2H), 2.64–2.74 (m, 1H), 3.83 (3H, s), 4.54 (d, *J* = 7.40 Hz, 1H), 4.62 (br s, 1H), 5.56 (br s, 1H), 6.53 (d, *J* = 8.5 Hz, 1H), 6.56–6.66 (m, 2H), 6.85–6.87 (m, 3H), 7.02–7.10 (m, 2H); ¹³C NMR (50 MHz, CDCl₃) δ: 23.4, 27.8, 31.0, 41.6, 55.9, 57.7, 57.9, 109.2, 113.7, 114.0, 117.6, 120.4, 128.9, 133.7, 144.7, 146.8, 147.3, 213.1; IR (cm⁻¹): 3474, 3353, 3052, 2936, 2866, 1700, 1604, 1500, 1325, 1265, 1234, 1033, 865, 746, 504; C₂₀H₂₃NO₃ (FW = 325.40): C, 73.82; N, 4.30; H, 7.12%; found: C, 73.54; N, 4.29; H, 7.13%; ESI-MS: *m/z* 324.2 [M – H]⁻.

Computational details

All calculations were carried out with the Gaussian 09 program³² using the M052X/6-311++G(d,p) theoretical model. It has been pointed out that “this method has the best performance for thermochemical kinetics, noncovalent interactions (especially weak interaction, hydrogen bonding, π···π stacking, and interaction energies of nucleobases), and the best composite results for energetics, excluding metals”.³³ The used triple split basis set adds p functions to hydrogen atoms and d functions to heavy atoms, in addition to diffuse functions to heavy atoms and hydrogens. The geometrical parameters of all stationary points in ethanol (ε = 24.3) were optimized using the conductor-like solvation model (CPCM).³⁴ The nature of all calculated structures was determined by frequency calculations: all positive eigenvalues for equilibrium structures, and one negative eigenvalue for transition states. The natural bond orbital analysis (Gaussian NBO version) was performed for all structures.

DPPH free radical scavenging assay

The free radical scavenging activity of the examined compounds was performed using the DPPH method, as described in ref. 35. Briefly, 1 mL (0.1 mM) solution of DPPH in methanol was added to an equal volume of the tested compound (20 μL of compound solution in DMSO and 980 μL of methanol) and left at room temperature for 20 and 60 min. After incubation the absorbance was recorded at 517 nm. As control solution, methanol was used. IC₅₀ is defined as the concentration sufficient to obtain 50% of a maximum scavenging capacity. All tests and analyses were run in triplicate and averaged. NDGA was used as an appropriate standard possessed 96% activity at 0.1 mM.

Cell preparation and culturing

The colon cancer adenocarcinoma cell line HCT-116 and breast cancer cell line MDA-MB-231 were obtained from the American Tissue Culture Collection (Manassas, VA, USA). These cells were propagated and maintained in DMEM and supplemented with 10% foetal bovine serum, and 100 IU mL⁻¹ penicillin and 100 μg mL⁻¹ streptomycin. The cells were grown in 75 cm² culture bottles and supplied with 15 mL DMEM until a

confluence of 70–80%. After a few passages the cells were seeded in 96-well plate and cultured in a humidified atmosphere with 5% CO₂ at 37 °C.

MTT assay for cell viability

Cell viability assay is based on the fact that MTT (3-(4,5-dimethylthiazol-2-yl)-2,5-diphenyltetrazolium bromide, a yellow tetrazole) is reduced to purple formazan in living cells. The absorbance of this coloured solution can be quantified spectrophotometrically. Cells were seeded in a 96-well plate (104 cells per well). After 24 h of incubation, the medium was replaced with 100 µl of each concentration (0.1, 1, 10, 50, 100 and 500 µM) of investigated Mannich bases for 24 and 72 h. Untreated cells served as a control. After 24 and 72 h of treatment, the cell viability was determined by MTT assay. The proliferation test is based on the colour reaction of mitochondrial dehydrogenase from living cells with MTT. At the end of the treatment period, MTT (final concentration 5 mg mL⁻¹ PBS) was added to each well, which was then incubated at 37 °C in 5% CO₂ for 3 h. The coloured crystals of the produced formazan were dissolved in 150 µL DMSO and the absorbance was measured at 570 nm on microplate reader (ELISA 2100C, Hamburg, Germany). Cell proliferation was calculated as the ratio of absorbance of the treated group divided by the absorbance of the control group, multiplied by 100 to give a proliferation percentage. The absorbance of the control group of cells served as viability of 100%.

Determination of superoxide anion radical (NBT assay)

The method is based on the reduction of nitrobluetetrazolium (NBT) to nitroblue-formazan in the presence of O₂^{•-}. Cells were seeded in a 96-well plate (104 cells per well). After 24 h of incubation, the medium was replaced with 100 µl of each concentration (1, 10, 50, and 100 µM) of investigated Mannich bases for 24 and 72 h. Untreated cells served as a control. After treatment and after proper incubation with the investigated compounds assay was performed by adding of 10 µL of 5 mg mL⁻¹ NBT to each well and then the cells were incubated for 3 h at 37 °C in 5% CO₂. To quantify the nitroblue-formazan product, which was solubilized in 10 µL DMSO and the resulting colour reaction was measured spectrophotometrically on microplate reader at 550 nm. The amount of reduced NBT was determined by the change in absorbance, based on molar extinction coefficient for monoformazan that is 15 000 M⁻¹ cm⁻¹.

Nitrite measurement (Griess assay)

Experiments were performed at room temperature. All samples were seeded also in triplicates in 96-well microtiter plate, incubated and treated as it was described in NBT assay. Equal volumes of 0.1% (1 mg mL⁻¹) *N*-(1-naphthyl)ethylenediamine and 1% (10 mg mL⁻¹) sulphanilic acid (solution in 5% phosphoric acid) to form the Griess reagent, were mixed together immediately prior to application to the plate. Briefly, the Griess reaction is a diazotization reaction in which the NO-derived nitrosating agent (*e.g.*, N₂O₃), generated from the acid-catalyzed formation of nitrous acid from nitrite (or the interaction of NO

with oxygen), reacts with sulphanilic acid to produce a diazonium ion that is then coupled to *N*-(1-naphthyl)ethylenediamine to form a chromophoricazo product that absorbs strongly at 550 nm. The absorbance at 550 nm was measured by using a microplate reader following incubation (usually 5–10 min). The results were expressed in nmol NO₂⁻/mL from a standard curve established in each test, constituted of known molar concentrations of nitrites.

Determination of reduced glutathione (GSH)

The used assay is based on the oxidation of reduced form of glutathione with reagent containing active thiol group, *i.e.* 5,5'-dithio-bis(2-nitrobenzoic acid) (DTNB) when a yellow product of 5'-thio-2-nitrobenzoic acid (TNB) is formed.³⁶ Experiments were performed at room temperature. Cells were seeded in triplicates on a 96-well plate (5 × 104 cells per well). The treatment was performed with 100 µl of the same concentrations of Mannich bases for 24 and 72 h as in NBT and Griess assays. Colour reaction was measured spectrophotometrically on microplate reader at 405 nm following incubation for 5 min. The results were expressed in nmol mL⁻¹ from a standard curve established in each test, constituted of known molar GSH concentrations.

Statistics

The data were expressed as mean ± standard error (SE). Biological activity was the result of 3 individual experiments, performed in triplicate for each dose. Statistical significance was determined using the Student's *t*-test or the one-way ANOVA test for multiple comparisons. A *p* value <0.05 was considered as significant. The magnitude of correlation between variables was done using SPSS (Chicago, IL) statistical software package (SPSS for Windows, version 17, 2008). The IC₅₀ values were calculated from the dose curves by a computer program (CalcuSyn).

Acknowledgements

This work was supported by the Ministry of Science and Technological Development of the Republic of Serbia (projects no. 172016, III41010).

Notes and references

- (a) T. P. Loh, S. Liung, K. Tan and L. L. Wei, *Tetrahedron*, 2000, **56**, 3227–3237; (b) P. Phukan, D. Kataki and P. Chakraborty, *Tetrahedron Lett.*, 2006, **47**, 5523–5525; (c) Y. Y. Yang, W. G. Shou and Y. G. Wang, *Tetrahedron*, 2006, **62**, 10079–10086; (d) T. Loh and S. Chen, *Org. Lett.*, 2002, **21**, 3647–3650; (e) K. K. W. Mak, J. Siu, Y. M. Lai and P. Chan, *J. Chem. Educ.*, 2006, **83**, 943–945.
- E. Takahashi, H. Fujisawa and T. Mukaiyama, *Chem. Lett.*, 2004, **33**, 936–937.
- (a) T. Akiyama, J. Takaya and H. Kagoshima, *Synlett*, 1999, **9**, 1426–1428; (b) T. Akiyama, K. Matsuda and K. Fuchibe, *Synlett*, 2005, 322–324; (c) K. Manabe, Y. Mori and S. Kobayashi, *Tetrahedron*, 2001, **57**, 2537–2544; (d)

- T. Akiyama, J. Takaya and H. Kagoshima, *Tetrahedron Lett.*, 2001, **42**, 4025–4028.
- 4 (a) L. Wang, J. Han, J. Sheng, H. Tian and Z. Fa, *Catal. Commun.*, 2005, **6**, 201–204; (b) W. B. Yi and C. Cai, *J. Fluorine Chem.*, 2006, **127**, 1515–1521.
- 5 (a) I. Ibrahim, W. Zou, J. Casas and A. Cordova, *Tetrahedron*, 2006, **62**, 357–364; (b) M. L. Kantam, C. V. Rajasekhar, G. Gopikrishna, K. R. Reddy and B. M. Choudary, *Tetrahedron Lett.*, 2006, **47**, 5965–5967.
- 6 (a) G. Zhao, T. Jiang, H. Gao, B. Han, J. Huang and D. Sun, *Green Chem.*, 2004, **6**, 75–77; (b) D. Fang, J. Luo, X. L. Zhou and Z. L. Liu, *Catal. Lett.*, 2007, **116**, 76–80; (c) J. Z. Li, Y. Q. Peng and G. H. Song, *Catal. Lett.*, 2005, **102**, 159–162; (d) S. Sahoo, T. Joseph and S. B. Halligudi, *J. Mol. Catal. A: Chem.*, 2006, **244**, 179–182; (e) A. C. Cole, J. L. Jensen, I. Ntai, K. L. T. Tran, K. J. Weaver, D. C. Forbes and J. H. Davis Jr, *J. Am. Chem. Soc.*, 2002, **124**, 5962–5963.
- 7 (a) A. Kumar and S. S. Pawar, *J. Org. Chem.*, 2004, **69**, 1419–1420; (b) A. P. Abbott, G. Capper, D. L. Davies, R. K. Rasheed and V. Tambyrajah, *Green Chem.*, 2002, **4**, 24–26; (c) A. Aggarwal, N. L. Lancaster, A. R. Sethi and T. Welton, *Green Chem.*, 2002, **4**, 517–520.
- 8 (a) D. Fang, K. Gong, D. Zhang and Z. Liu, *Monatsh. Chem.*, 2009, **140**, 1325–1329; (b) K. Gong, D. Fang, H. L. Wang and Z. L. Liu, *Monatsh. Chem.*, 2007, **138**, 1195–1198; (c) C. B. Yue, T. F. Yi, C. B. Zhu and G. Liu, *J. Ind. Eng. Chem.*, 2009, **15**, 653–656.
- 9 (a) D. Yin, C. Li, L. Tao, N. Yu, S. Hu and D. Yin, *J. Mol. Catal. A: Chem.*, 2006, **245**, 260–265; (b) Y. Xiao and S. V. Malhotra, *J. Mol. Catal. A: Chem.*, 2005, **230**, 129–133.
- 10 (a) I. Cota, R. Gonzalez-Olmos, M. Iglesias and F. Medina, *J. Phys. Chem. B*, 2007, **111**, 12468–12477; (b) M. Iglesias, R. Gonzalez-Olmos, I. Cota and F. Medina, *Chem. Eng. J.*, 2010, **162**, 802–808.
- 11 X. S. Zhou, J. B. Liu, W. F. Luo, Y. W. Zhang and H. Song, *J. Serb. Chem. Soc.*, 2011, **76**, 1607–1615.
- 12 (a) B. B. Toure and D. G. Hall, *Chem. Rev.*, 2009, **109**, 4439–4486; (b) M. Arend, B. Westermann and N. Risch, *Angew. Chem., Int. Ed.*, 1998, **37**, 1044–1070; (c) A. Izumiseki, K. Yoshida and A. Yanagisawa, *Org. Lett.*, 2009, **11**, 5310–5313; (d) A. Córdova, *Acc. Chem. Res.*, 2004, **37**, 102–112; (e) S. N. Pandeya, V. S. Lahshmi and A. Pandeya, *Indian J. Pharm. Sci.*, 2002, **65**, 213–222.
- 13 S. Joshi, N. Khosla and P. Tiwari, *Bioorg. Med. Chem.*, 2004, **12**, 571–576.
- 14 F. Lopes, R. Capela, J. O. Goncaves, P. N. Horton, M. B. Hursthouse, J. Iley, C. M. Casimiro, J. Bom and R. Moreira, *Tetrahedron Lett.*, 2004, **45**, 7663–7666.
- 15 M. G. Ferlin, G. Chiarelto, F. Antonucci, L. Caparrotta and G. Frolidi, *Eur. J. Med. Chem.*, 2002, **37**, 427–434.
- 16 (a) B. S. Holla, B. Veerendra, M. K. Shivananda and B. Poojary, *Eur. J. Med. Chem.*, 2003, **38**, 759–767; (b) K. Kucukoglu, M. Gul, M. Atalay, E. Mete, C. Kazaz, O. Hanninen and H. I. Gul, *Arzneim. Forsch.*, 2011, **61**, 366–371; (c) H. I. Gul, J. Vepsalainen, M. Gul, E. Erciyas and O. Hanninen, *Pharm. Acta Helv.*, 2000, **74**, 393–398; (d) J. R. Dimmock, E. Erciyas, S. K. Raghavan and D. L. Kirkpatrick, *Pharmazie*, 1990, **45**, 755–757.
- 17 W. Malinka, P. Swiatek, B. Filipek, J. Sapa, A. Jerierska and A. Koll, *Farmaco*, 2005, **60**, 961–968.
- 18 M. Kouskoura, D. Hadjipavlou-Litina and M. Giakoumakou, *Med. Chem.*, 2008, **4**, 586–596.
- 19 H. I. Gul, T. Ojanen, J. Vepsalainen, M. Gul, E. Erciyas and O. Hanninen, *Arzneim. Forsch.*, 2001, **51**, 72–75.
- 20 D. H. Park, J. Venkatesan, S. K. Kim, V. Ramkumar and P. Parthiban, *Bioorg. Med. Chem. Lett.*, 2012, **22**, 6362–6367.
- 21 (a) C. Mukhopadhyay, A. Datta and R. J. Butcher, *Tetrahedron Lett.*, 2009, **50**, 4246–4250; (b) Y. S. Wu, J. Cai, Z. Y. Hu and G. X. Lin, *Tetrahedron Lett.*, 2004, **45**, 8949–8952.
- 22 D. Simijonović, Z. D. Petrović and V. P. Petrović, *J. Mol. Liq.*, 2013, **179**, 98–103.
- 23 T. Mosmann, *J. Immunol. Methods*, 1983, **65**, 55–63.
- 24 J. V. Košarić, D. M. Cvetković, M. N. Živanović, M. G. Čurčić, D. S. Šeklić, Z. M. Bugarčić and S. D. Marković, *J. Buon*, 2014, **19**, 283–290.
- 25 C. Auclair and E. Voisin, Nitrobluetetrazolium reduction, in *Handbook of Methods for Oxygen Radical Research*, ed. R. A. Greenwald, CRC Press, Inc, Boca Raton, 1985, pp. 122–132.
- 26 (a) P. Griess, *Ber. Dtsch. Chem. Ges.*, 1879, **12**, 426–428; (b) D. A. Wink and J. B. Mitchell, *Free Radicals Biol. Med.*, 1998, **25**, 434–456.
- 27 I. Fridovich, *Arch. Biochem. Biophys.*, 1986, **247**, 1–11.
- 28 S. Zheng, F. Yumei and A. Chen, *Free Radicals Biol. Med.*, 2007, **43**, 444–453.
- 29 J. Dai and R. J. Mumper, *Molecules*, 2010, **15**, 7313–7352.
- 30 Y. Murakami, A. Hirata, S. Ito, M. Shoji, S. Tanaka, T. Yasui, M. Machino and S. Fujisawa, *Anticancer Res.*, 2007, **27**, 801–808.
- 31 (a) M. Kaczmarek, M. Frydrychowic, A. Nowicka, M. Kozłowska, H. Batura-Gabryel, J. Sikora and J. Zeromski, *J. Physiol. Pharmacol.*, 2008, **59**, 321–333; (b) M. Higashiyama, J. Okami, J. Maeda, T. Tokunaga, A. Fujiwara, K. Kodama, F. Imamura and H. Kobayashi, *J. Thorac. Dis.*, 2012, **4**, 40–47.
- 32 M. J. Frisch, W. G. Trucks, B. H. Schlegel, E. G. Scuseria, A. M. Robb, R. J. Cheeseman, G. Scalmani, V. Barone, B. Mennucci, A. G. Petersson, H. Nakatsuji, M. Caricato, X. Li, P. H. Hratchian, F. A. Izmaylov, J. Bloino, G. Zheng, L. J. Sonnenberg, M. Hada, M. Ehara, K. Toyota, R. Fukuda, J. Hasegawa, M. Ishida, T. Nakajima, Y. Honda, O. Kitao, H. Nakai, T. Vreven, A. J. Montgomery Jr, E. J. Peralta, F. Ogliaro, M. Bearpark, J. J. Heyd, E. Brothers, N. K. Kudin, N. V. Staroverov, R. Kobayashi, J. Normand, K. Raghavachari, A. Rendell, C. J. Burant, S. S. Iyengar, J. Tomasi, M. Cossi, N. Rega, J. M. Millam, M. Klene, J. E. Knox, J. B. Cross, V. Bakken, C. Adamo, J. Jaramillo, R. Gomperts, E. R. Stratmann, O. Yazyev, J. A. Austin, R. Cammi, C. Pomelli, W. J. Ochterski, L. R. Martin, K. Morokuma, G. V. Zakrzewski, A. G. Voth, P. Salvador, J. J. Dannenberg, S. Dapprich, D. A. Daniels, O. Farkas, B. J. Foresman, V. J. Ortiz, J. Cioslowski and J. D. Fox, *Gaussian 09*, Rev A.1 Gaussian Inc., Wallingford, 2009.

- 33 Y. Zhao, N. E. Schultz and D. G. Truhlar, *J. Chem. Theory Comput.*, 2006, **2**, 364–382.
- 34 (a) V. Barone and M. Cossi, *J. Phys. Chem. A*, 1998, **102**, 1995–2001; (b) M. Cossi, N. Rega, G. Scalmani and V. Barone, *J. Comput. Chem.*, 2003, **24**, 669–681.
- 35 C. Kontogiorgis and D. Hadjipavlou-Litina, *J. Enzyme Inhib. Med. Chem.*, 2003, **18**, 63–69.
- 36 M. A. Baker, G. J. Cerniglia and A. Zaman, *Anal. Biochem.*, 1990, **190**, 360–365.